Scientific Research Publishing

Engineering, 2021, 13, 707-738
https://www.scirp.org/journal/eng
ISSN Online: 1947-394X
ISSN Print: 1947-3931

A New Approach to Analyzing Behavioral Change Propagation in Redesigning of Drone Camera Stabilizer

Hamid Reza Moghadas Najaf Abad, Ali Mahmoodi*, Farshad Pazooki

Department of Aerospace Engineering, Faculty of Engineering, SRBIA University, Tehran, Iran
Email: h.r.moghadas@gmail.com, *ali.mahmoodi@srbiau.ac.ir, pazooki_fa@srbiau.ac.ir

How to cite this paper: Moghadas Najaf Abad, H.R., Mahmoodi, A. and Pazooki, F. (2021) A New Approach to Analyzing Behavioral Change Propagation in Redesigning of Drone Camera Stabilizer. *Engineering*, **13**, 707-738.
https://doi.org/10.4236/eng.2021.1312051

Received: September 26, 2021
Accepted: December 28, 2021
Published: December 31, 2021

Abstract

Redesigning of complex products is not an easy task. Engineering change requirements can be extracted at any stage of the product redesign process, and it makes the management of engineering change become a challenging mission. The motivation for this study is to find the shortest path of behavioral change propagation (BCP), minimize the BCP, access to the special behavioral elements in order to better managing the BCP and classifying the behavioral attribute of the elements in terms of their relationship to change by betweenness centrality coefficient (BNCC), clustering coefficient (CLC), reachability coefficient (RC) and change propagation index (*CPI*). In this article, the procedure of managerial decision-making is proposed by combining system restrictions in behavioral clustering design structure matrix (BCDSM) with optimization algorithms. The practicality of suggested method is verified in redesign procedure of a phantom drone camera stabilizer as a case study. The results, indicate that the absorption of change by behavioral elements is dominant in the mechanical (63.9%), electrical (61.1%) and thermal (38.9%) behaviors of the drone camera stabilizer system in redesign process. These elements are best candidates for reducing the cost and time of behavioral changes in the system redesign and are desirable for the designer.

Keywords

Behavioral Change Propagation, Behavioral Clustering Design Structure Matrix, Drone Camera Stabilizer

1. Introduction

The change propagation, is one of the most important issues in engineering. It should be taken into the account in conceptual design, manufacturing and even

in after sale services. In designing of a product, the changes propagate considerably make an impact in product development [1] [2]. A well-known example is the one experienced by "Smart Tool Lab" on a passenger car in which the change propagation is traced from a small change in rear window up to front bumper [3]. At first the change in inclination of rear window seems to be completely irrelevant to the shape and size of the front bumper, however insight into it, appears the chain of relationships between these two objects.

Consideration a simplified approach in which a product with a 2D drawing with two-step prediction method for change propagation is proposed [4]. An optimization has been added to that model, finding the shortest path algorithm in most time-saving paths for propagating changes dependent on other design tasks [5]. A new approach to managing change control is presented in the design process of complex engineering products by use of design constraints in a combination of two structures of DSM matrices and a systematic process for controlling changes [6]. A decision support for manufacturing change management is provided to enable a thorough analysis of change in socio-technical manufacturing systems [7]. An integrated approach for scheduling design changes in the complex product development process is presented by combining simulation of change propagations with optimization algorithms [8]. The dynamics of a stable 3-axis gyroscopic plate is investigated and analyzed by considering the angular movements of its carrier body [9]. The dynamical modeling of a gyro stabilized platform is studied in the presence of angular motions of the vehicle [10]. The computer aided design (CAD) management model, which enables us to better managing the digital mockup (DMU) and propagate changes to the hole assembly after a modification that affects one of its component, that has been modified and sent to a partner and then reinserted is explained [11]. A case study approach to study engineering change (EC) and its propagation in the context of a university design project is used as an example of young organizations and is compared with the existing work done on mature firms [12]. Three engineering systems as networks and measure the relation between modularity and robustness to random failures are modeled to that end whether modularity comes at the expense of robustness [13]. Four types of network models of systems, component-component, component-function, component-parameter, and function-parameter, to further test the relation of robustness to the type of system representation, architectural or behavioral are produced.

The relevant learnings about inter-team coordination can be made from non-software development [14]. To illustrate this an example of mechanical integration engineers and their work in large-scale and complex hardware development is provided. The two perspectives are joined by analyzing metadata of more than 3000 documents produced during the design of a biomass power plant [15]. The insights are gained by using network analysis and by visualizing the temporal unfolding of the design process. A new method is presented for analyzing requirement change propagation [16]. This method is based on the

assessment of requirement interrelations structured in a requirements structure matrix by a modified page-rank algorithm. By this method, a high number of strongly interrelated requirements can be analyzed in an efficient manner.

The strengths of this research compared to similar research are: in most of the work done, less control and management of engineering changes in the important phases of redesign has been done, while in the current research, the focus is on redesign. Combining behavioral matrices and creating a BCDSM matrix that creates a sensitivity matrix by combining product behaviors. This matrix helps the surgeon predict growth changes [4]. Relying on the knowledge of the chief designer in parallel with the change management [6] software is very effective in managing the growth of change and achieving the most optimal path of change. Flexible to implement in complex engineering projects [8]. Define several indicators to quantify change growth management and select the most optimal change path.

In this paper, a plan for management of BCP is proposed. The following reasons make products complicated form redesigning point of view:

1) They contain a plenty of systemic parameters.
2) There are a lot of relationships between different components.
3) Finding the relationships between components needs technical knowledge.
4) The parameters relations are complicated.
5) There are so much restrictions in design and manufacturing.

This study concentrates on following items:

- Developments of behavioral changes in redesign (growth of behavioral changes in redesign)
- Manageability in product lifecycle management (PLM) [1] [2]
- Management of behavioral changes in redesign
- Finding the relationships between subsystems and components
- Management of behavioral changes of complex products [8]

The probabilities and effects of behavioral changes between system components are stored in the BCDSM to determine and detect the variability of a complex engineering system [8]. In this paper, BCDSM matrices are used as a combination of behavioral properties. The reason for using a combinatorial matrix is to access easier control of changes for such a complex product [8].

2. Materials and Methods

2.1. Management of Behavioral Changes Methodology

In this paper, the methodology proposed for management of behavioral changes is based on six foundations as follows:

- BCDSM, which describes the relationship between behavioral parameters
- Determination and constructing constraint levels of behavioral parameters in redesign
- Evaluation of engineering changes, which estimating the volume of communication between BCDSM matrix behavioral parameters and identification of

the sensitivity range of all behavioral parameters

- Propagation model between behavioral parameters
- Measuring the behavioral changes from behavioral change management [6] center (BCMC) point of view
- Comprehensive (Genetic Algorithm) GA for management of behavioral changes

The relationship between structural features of products and behavioral features are explained and arranged in format of BCDSM matrix. The matrix containing these two kinds of relationships, called the BCDSM, which is shown in **Figure 1**.

In **Figure 1**, the off-diagonal first level behavioral parameters contain the parameters that connect the subsystems or known components in the diagonal blocks in the larger matrix to the 2nd level off-diagonal behavioral parameters contain the ones that link the different behavioral properties within the diagonal blocks in the larger matrix. Selecting such a BCDSM the designer simplify the relationships between behavioral changes management. Sensitivity analysis [16] of behavioral changes of redesign to should simultaneously be developed with the redesign process. As the redesign process goes ahead, the process of sensitizing behavioral changes to affected behavioral properties should also proceed. Failure in this procedure may lead to not closure of the behavioral change loop and ultimately leads to consumed time and cost and even project failure [15].

A behavioral change in any of the first level behavioral parameters can lead to a behavioral change in the other first level parameters as well as the 2nd level behavioral parameters in proportion to the first level parameters. At the same time, by considering the constraints, a method can be developed so that satisfies all the requirements of the behavioral changes. Of course, in the development of this model, the main task of the Camera Gyro Stabilizer (CGS) designer would be difficult and requires high level of technical knowledge [9] [10]. Without such knowledge, working with this model would be very time consuming and expensive. **Figure 2** shows the algorithm of the above mentioned method. The steps of the method consist of three parts as follows:

- Part I, Sensitivity: in this part, sensitization of all behavioral parameters within the BCDSM to each other is performed. The relationship between behavioral parameters are expressed as some equations known as system equations are for expressing the relationship between first level behavioral parameters and subsystem design equations are to express the relationship between subsystem behavioral parameters. In this section, the range of change of all system behavioral parameters due to the change of one behavioral parameter is calculated.
- Part II, Redesign: in this part, a large volume of relationships are used in the complex system redesign process [8]. Using the system equations is used to express the relationship between first level behavioral parameters and subsystem design equations the relationship between subsystem behavioral parameters and the relationship between the behavioral parameters affecting

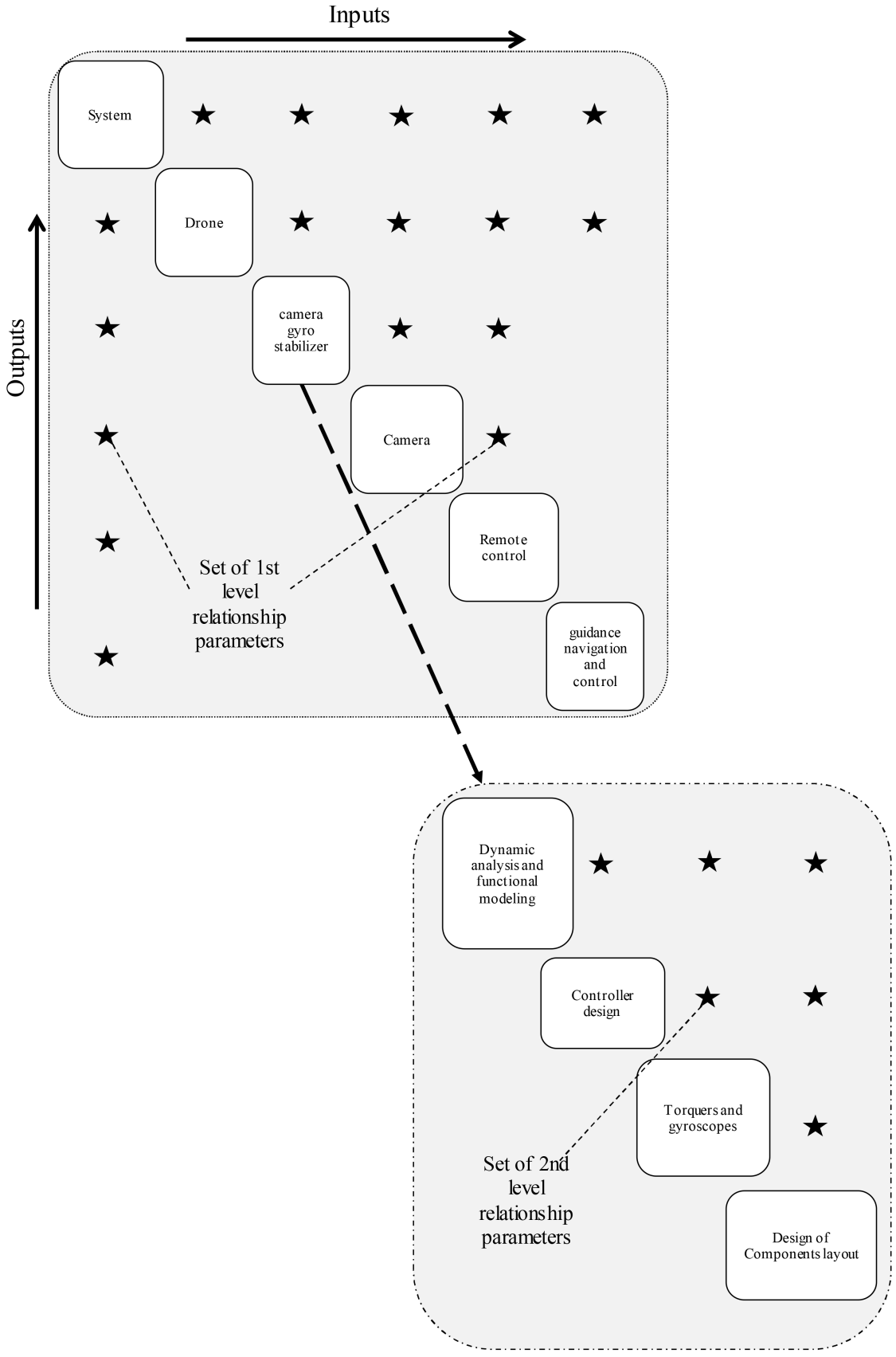

Figure 1. BCDSM for 3-axis drone camera gyro stabilizer.

each other is determined and shows the extent of change of all system behavioral parameters due to the change of one parameter.

- Part III, Integrating: in this section, the relationship between all the behavioral parameters of the first level and the 2nd level is applied to the redesign process and the minimum changes of the behavioral parameters relative to the changed parameter are obtained. The main output of the software is the results of reviewing behavioral changes.
- Part IV, behavioral Change Management [6] Center (BCMC) Review: in this part, the designer achieves his desired results according to the algorithm shown in **Figure 2**.

2.2. BCP Model

It is very difficult to find the right path of BCP in the process of management of behavioral changes in the presence of complex relationships. In order to create a proper transmission trace of behavioral changes in complex systems, in addition to the need for the knowledge of the chief designer, the knowledge of the designer of the subsystems and system tools is needed to create an integrated model [8] of the behavioral change transfer algorithm. The algorithm for creating a propagation model for complex systems is shown in **Figure 3**.

According to the flowchart of **Figure 3**, the structure of the BCP algorithm is obtained as a result of the designer's expertise and utilization of:

- Cambridge advanced modeller (CAM) software [14] code, which determines the range of behavioral change resulting from the change
- Integrating of design algorithm to create integrated [8] relationships between first level parameters
- BCDSM matrix as a roadmap for all possible relationship paths between behavioral parameters

Also, the knowledge of management of subsystem changes is obtained as a result of the expertise of subsystem designers and utilization of:

- BCDSM matrix of behavioral properties for each of the subsystems
- Integrating of design algorithm software to create integrated [8] relationships between 2nd level parameters of two subsystems
- Analysis of laboratory and engineering tests [16]

For each change request, knowledge of change management [6] at the system and subsystem level leads to a system change management algorithm [6]. The possible paths obtained by trade-off using these algorithms together and the Integrating between Information circulations creates the subsystem propagation model.

2.3. Behavioral Change Management Center (BCMC)

In the redesign phase, it is not possible to define a preset process for the amount of workload. Therefore, to define the cost, time and workload of all behavioral changes, the BCMC needs to achieve different types of impact [7] on a behavioral

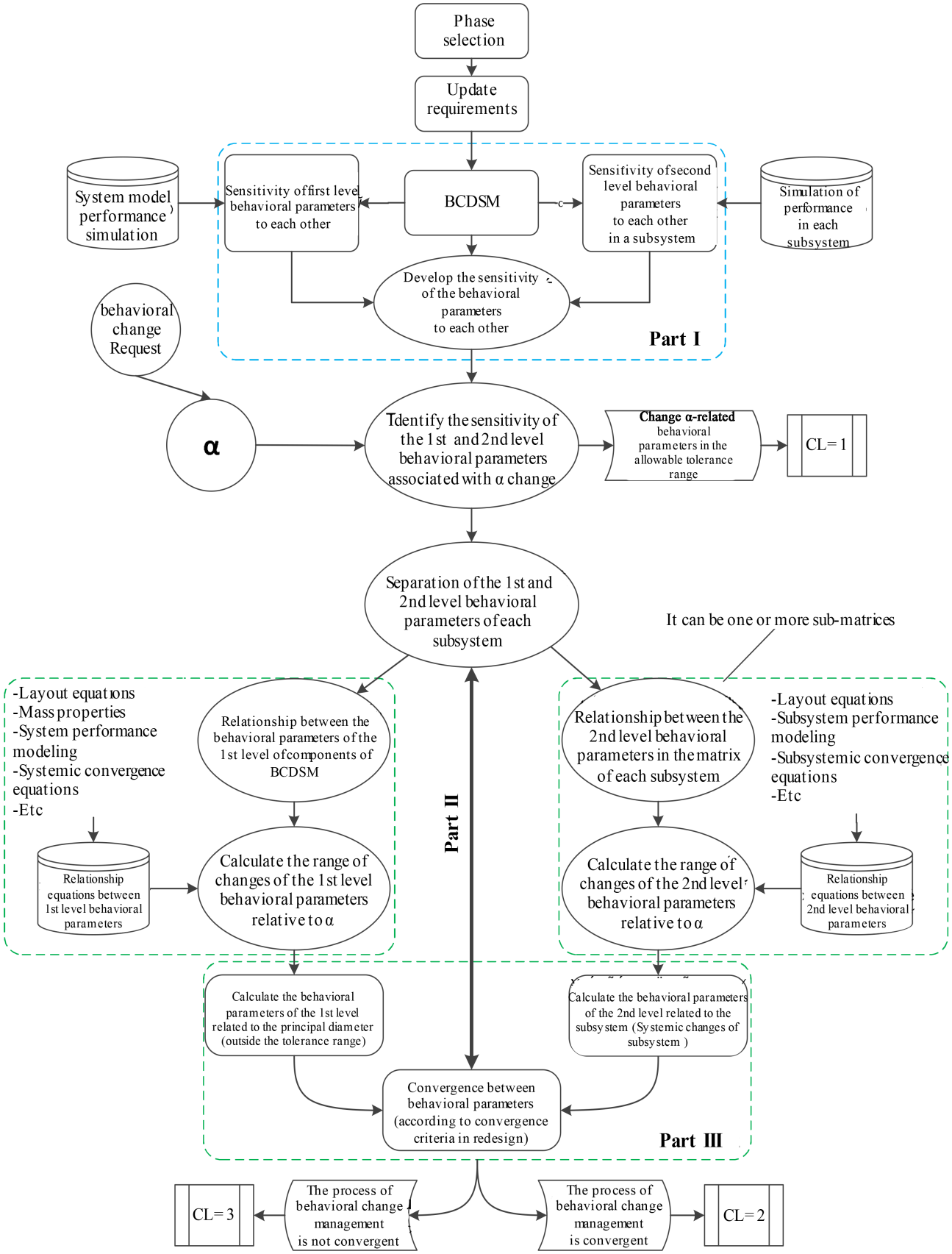

Figure 2. Algorithm for evaluating behavioral changes in the redesign process.

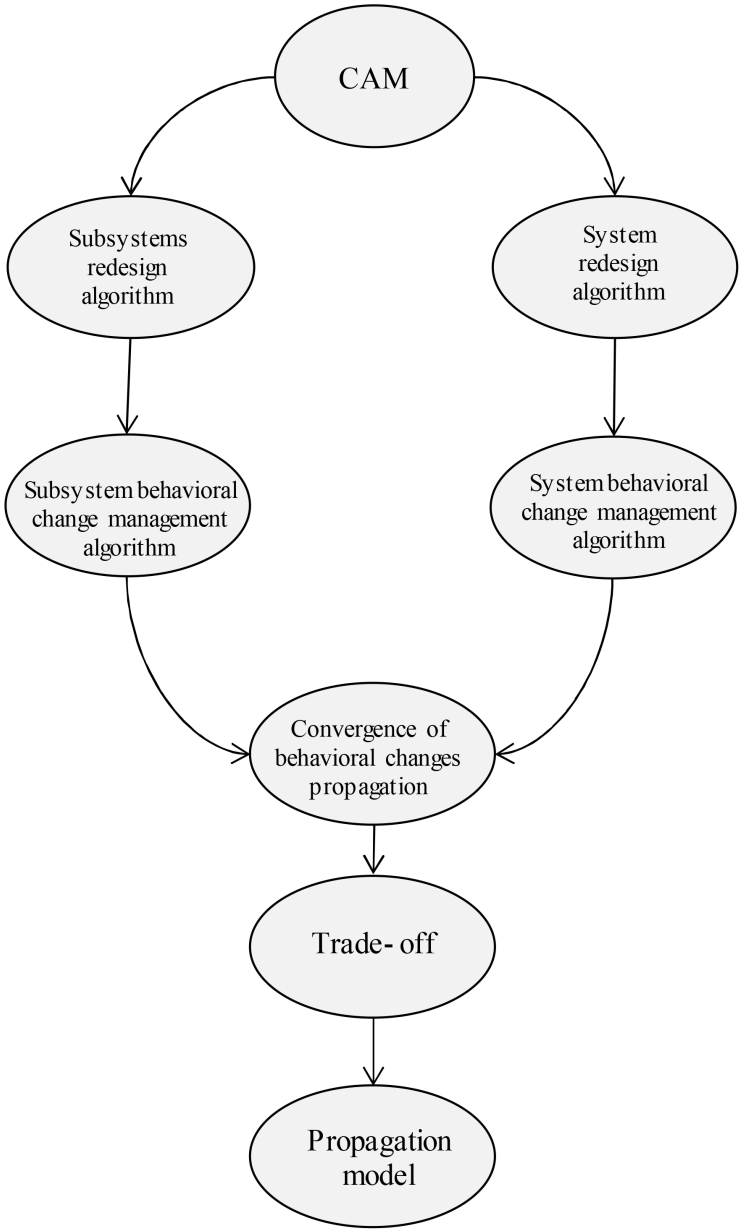

Figure 3. BCP model.

change in the product life cycle. Questions and the effect of each following items should be specified for the BCMC:

- Is this behavioral change to improve requirements?
- Is this behavioral change due to redesign constraints such as assembly problems [11]?
- Is this behavioral change due to low level of technology readiness levels (TRLs), lower cost or inability to purchase some parts?
- Is this behavioral change due to other changes in the product?
- Is this an exigent behavioral change and should it be done?

To quantify these questions, the relationships in **Table 1** are used. The following points should be considered for using **Table 1**:

Table 1. Effect number index.

producer	Symbol and impact number	Coefficient name
Chief Designer	a (1..4)	Workload
project manager	b (1..4)	Consumer resources
Related specialists	c (1..4)	Time
Chief Designer/Simulator person	if $+ \rightarrow d$ (0.25..1) $- \rightarrow d$ (1..4)	Improve of requirements
project manager	if $+ \rightarrow f$ (0.1..1) $- \rightarrow f$ (1..2)	exigent

- The selection of the amount of impact number [7] is done qualitatively by the relevant people.
- Values greater than 1 indicate a greater impact intensity, and values less than 1 lead to positive effects of behavioral change.
- The workload coefficient is obtained by the chief designer after using the CAM software [14].
- The coefficient of resource consumption is determined by the project manager after announcing the opinion of the involved parts [15].
- The time coefficient is determined after announcing the time required for each sub-section to perform its specific behavioral properties.
- Requirement improvement coefficient is obtained after reviewing the designer or the person responsible for performance analysis [16] (simulator person) in order to influence the behavioral change on the improvement of requirements according to the customer.
- The exigent coefficient is obtained according to the forced effect of a behavioral change to remove the exigent or the lack of suitable materials and parts or etc.

The probability value of the effect is obtained from the following relation:

$$\mathrm{POE} = a \times b \times c \times d \times f \tag{1}$$

$$\mathrm{TAC} = b \times c \tag{2}$$

Depending on the value of the probability of effect (POE) parameter and the time and cost (TAC) of consumption, can be made quantitatively for managerial decision making for a behavioral change. POE quantifies the impact [7] of the requested behavioral change on the project [15], and TAC quantifies the amount of time and cost.

2.4. Behavioral Change Management Algorithm

A behavioral change request can be made by any of the subsystems. This request is made for one of the following reasons:

- Growth of structure failure in redesign
- Reduction of costs

- Layout and location constraints
- Improvement of customer requirements
- Optimization in redesign

In the first step, the behavioral change request is sent to the BCMC, and this center examines the behavioral change request according to the effectiveness of the change. Follow-up and implementation of behavioral change management [6] algorithm according to **Figure 4**, is done by the BCMC. This algorithm is performed according to the needs of the project manager, system chief designer and personnel engaging the project [15]. The comprehensive GA for behavioral change management [6] consists of five main parts:

1) Configuration and sensitization of all matrix elements regarding each other
2) Constrain levels of each part of a redesign phase
3) Using CAM software [14]
4) Trade-off Propagation method (Propagation Model)
5) Management evaluation in order to PLM.

2.5. Application of the Suggested Method to a Case Study

CGSs are gyroscopic devices that are applied for stabilizing a variety of instruments and equipment on moving objects [9] [10]. This is done by a closed-loop feedback control system which detects the error of orientations and tries to diminish this errors. These devices are also used to measure the deflection angles of flying objects. These include directional and vertical gyroscopes and 3-axis positioning systems based on CGSs. There are various instruments and equipment in CGS which should be stabilized such as: accelerometers of the inertial navigation system, cameras mounted on flying objects, astronomical navigation blocks, and so on [9] [10].

From the stabilization point of view, CGSs are divided into active and passive types, and from the mission point of view, they are divided into types of force and indicator, in the sense of degrees of freedom of devices against angularly stabilization, they are divided into one, two and 3-axis types. In this regard, the control system of a 3-axis CGS stabilizes and controls all three axes of the body in space [9] [10].

From the stabilization point of view, CGSs are classified into two types: passive and active. **Figure 5** shows different types of CGSs for camera stabilization.

The passive (or uniaxial) type basically consists of a three-degree free gyroscope that neutralizes the annoying torques applied to the object attached to its outer frame by moving forward around its inner frame axis, producing gyroscopic torque. Here, gyroscopic rigidity and gyroscopic precession principle will be of great importance. Due to the inherent defect in the passive CGS, *i.e.* the loss of the stabilizing properties of the gyroscope at a deviation of about 90 degrees, an actuator helps the gyroscope become stable through the feedback circuit in which case an active CGS will be obtained. In this type of CGS a regulator control system returns the precision axes to their initial position by utilization of

pickoff sensors or shaft encoders as the measurement devices of angular deviations. This keeps the precession axis of gyroscope close to zero or eliminating the annoying external torques. This type of CGS is also called "force CGS". Compared to a force CGS, it is an indicator type which is an active CGS and due to its gyroscope type, it does not produce gyroscopic torque at all. In this type of CGS, the gyroscope is mounted on the stability axis and directly measures the deviation

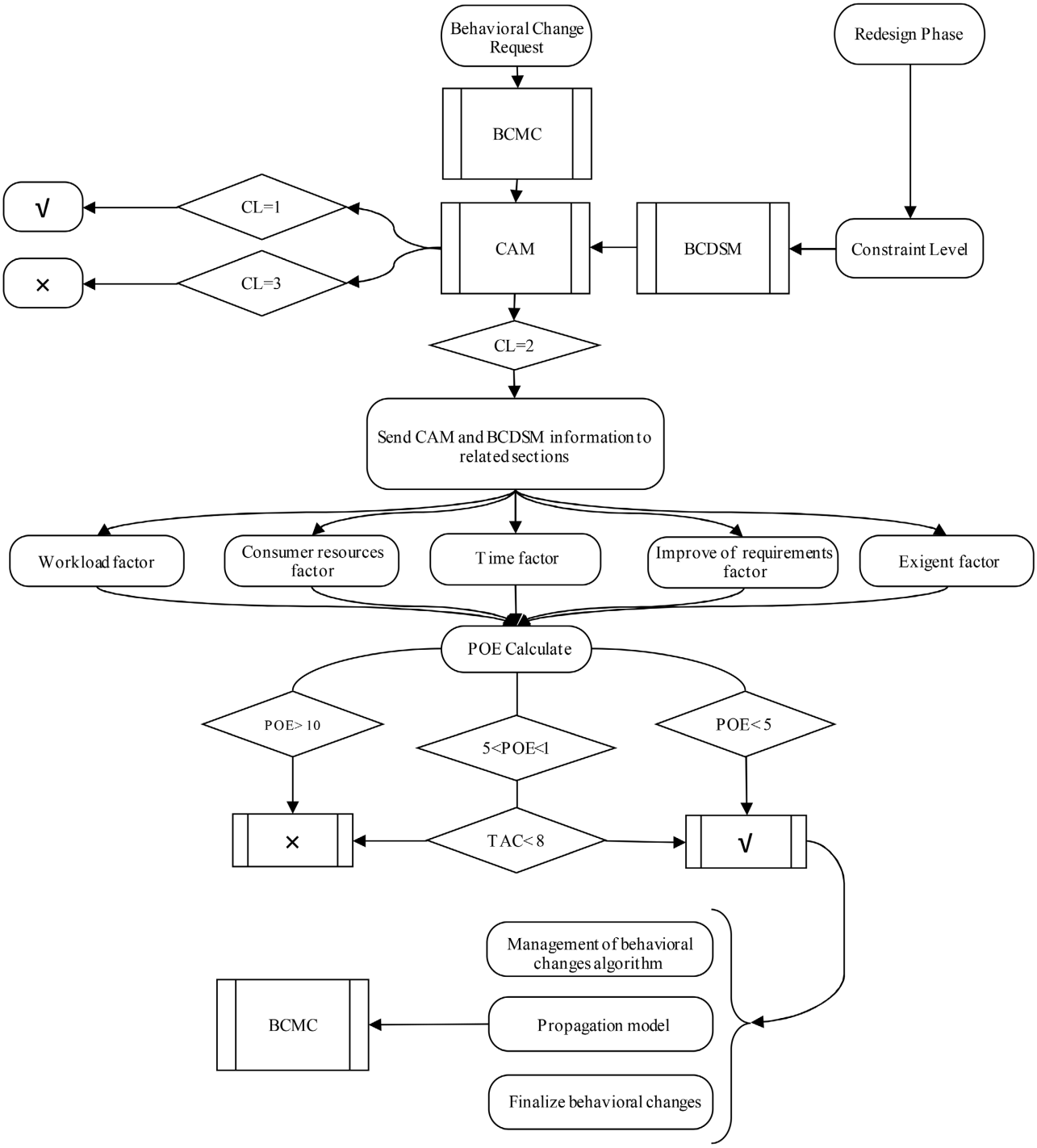

Figure 4. Comprehensive algorithm for management of behavioral changes.

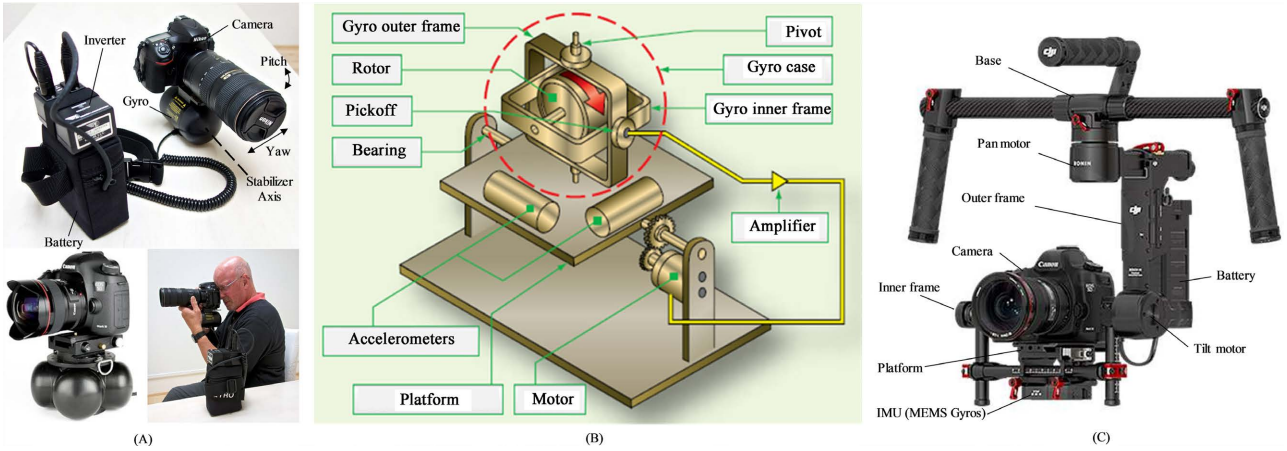

Figure 5. Different types of CGSs for camera stabilization. (A) Passive; (B) Active (Force CGS); (C) Active (Indicator CGS). (Adapted from, respectively: https://luminous-landscape.com/kenyon-labs-gyro-stabilizer/www.flightliteracy.com/inertial-navigation-system-ins-part-one/cheesycam.com/custom-pelican-hard-case-for-dji-ronin-m-gimbal-1uas-carry-on-size/).

of the stability angle from zero and based on this, the command creating control torque is delivered by the feedback circuit. Here, the task of eliminating the external annoying torque is only the responsibility of the torque generator motor. Based on what has been said about indicator CGS, feedback circuits, especially torque motors, must be of very high accuracy and quality to ensure proper stability accuracy, in the event that, in the force CGS, there is less need for motors with very high accuracy and quality. 3-axis CGSs can be divided into two categories based on the type of structure: with platform and without platform [9] [10]. Either of above mentioned types has advantages and disadvantages. Advantages and Disadvantages of CGS systems with platform are as follows:

Advantages of CGS systems with platform are as follows:

1) Simpler gyros. Because the sensor platform rotates only at small rates needed to keep it level, the gyros need only a small dynamic range. A maximum rate of 3 degree/s would suffice for a gyro of 0.01 degree/h performance (e.g., for an aircraft navigator), a range of 10^6. Further, gyro torque errors do not lead to attitude error. The lack of gyro rotations means that there are no aniso inertia and output axis angular acceleration errors to minimize in the design.

2) Higher accuracy. Because the accelerometer axes are always well defined, the platform navigator can be very accurate; the North and East accelerometers see no component of gravity and measure only the vehicle accelerations. The vertical accelerometer, though, measures the vehicle's vertical motion in the presence of 1 g, therefore less accurately. In an aircraft this causes altitude errors, which can be compensated with a barometer signal.

3) Self-alignment by gyro compassing.

4) Sensor calibration by platform rotations. The other sensor biases are obtained by orienting the platform with each major axis vertical in turn, provided there is enough time.

Disadvantages of CGS systems with platform are as follows:

1) Complexity and cost. The gimbal structure and its bearings must be stiff so that the accelerometer axes remain defined even under vehicle vibrations, but the bearings and slip rings must have as little friction as possible. As a result, the gimbal structure is an elaborate, precisely made, expensive, mechanism.

2) Gimbal magnetics. Each gimbal must have a pickoff and torque. The pick-offs (synchros) measure the inter gimbal angles with arc-sec resolution over a full revolution, a range of 10^6. When the system is first switched on, the torquers need to provide enough torque to accelerate the platform inertia so that it can gyrocompass and align itself to Level and North in a reasonable time. The torquers also must not leak magnetic flux, for that could upset the sensors as the gimbals move around them.

3) Reliability. The bearings and slip rings tend to wear, degrading alignment and performance.

Advantages and Disadvantages of Strap-down (CGS systems without platform) are as follows:

Advantages of Strap-down systems are as follows:

1) Simple structure, low cost. Strap-down systems are lighter, simpler, cheaper, and easily configured for odd-shaped spaces. As it is only necessary to mount the sensors so that their sensing axes point in known directions (usually orthogonal) in the vehicle, they can be placed so that they best use the space available.

2) Ruggedness. The simpler structure better withstands shock and vibration, and, because it is lighter, it is easier to shock mount than a platform.

3) Reliability. There are no gimbal magnetics, no slip rings, and no bearings. The electronics that replace them are inherently more reliable.

Disadvantages of Strap-down systems are as follows:

1) Alignment. Strap-down systems are difficult to align because they cannot be easily moved. Transfer alignment is suitable for tactical systems.

2) Sensor calibration. Again, the immobility means that the sensors cannot be calibrated in the system. Therefore, they must be stable, a burden on the sensor design. Strap-down systems rely on sensor models, using real-time compensation of inertial errors and thermal effects.

3) Motion-induced errors. The body motions induce unique sensor errors (torque errors, anisoinertia, output axis angular acceleration), which can be compensated to some degree.

4) Accelerometer errors. Bias errors accumulate, and Strap-down accelerometers may be subjected to components of gravity as the vehicle rolls and pitches, reducing the accuracy of the vehicle acceleration measurement and exciting cross-axis errors.

5) The Strap-down computer. Not needed in the platform system, the computer must be fast enough to do all the Strap-down calculations in a few milliseconds. In a typical system, a bandwidth of 100 Hz demands that sensor compensation and coordinate transformation must be done in less than 0.01 s. This requires well-crafted program code.

Based on above mentioned materials, active CGSs use a control feedback cir-

cuit that drives a servo motor to react to external disturbances according to relationships and properties and return the platform to its stable state. For this purpose, the inertia between the inner and outer frame should be in acceptable range so that make the overall system stabilizable. This will be too complicated for a 3-axis CGS that has coupled equations for three axes of stability [9] [10]. **Figure 6** shows how to determine the behavioral elements for the phantom drone CGS. There are (32 × 3) = 96 the behavioral element which is defined using three behavioral characteristics: mechanical (Me), electrical (El) and thermal (Th). Behavioral links between these 96 elements are first recorded in the design structure matrices related to the behavioral properties and then together in a behavioral design structure matrix.

A right hand side coordinate system that includes the relationships of all members of the gyroscopic stabilization system is shown in **Figure 7** [9] [10]. The axes X_P, Y_P and Z_P are related to the platform, and X_I, Y_I and Z_I are related to the inner frame, the coordinates X_O, Y_O and Z_O are related to the outer frame and the coordinates X_G, Y_G and Z_G are related to the base. The members of this CGS are assumed to be rigid. The angles and the angular velocities of members are defined as follows [9] [10]:

θ: The relative angle between the inner frame and the platform, which is measured about the Y axis of the platform(Y_P).

ψ: The relative angle between the outer and inner frames that is measured about the Z axis of the inner frame(Z_I).

ϕ: The relative angle between the outer frame and the base that is measured about the X axis of the outer frame(X_O).

The angles and the angular velocities defined above follow an Euler sequence of 1, 2, 3 (ϕ, ψ, θ) starting at the base and ending at the platform.

Each member of the system behaves as a rigid body. The net torque applied to each frame includes the torque applied to that frame by the adjacent outer frame and the reaction torque by the inner frame adjacent to that frame (See **Figure 5(B)** & **Figure 5(C)**). The corresponding equations are expressed in the coordinate system for each member. Adjacent members and frames are defined according to **Figure 7**. The dynamic equations of the system are written in such a

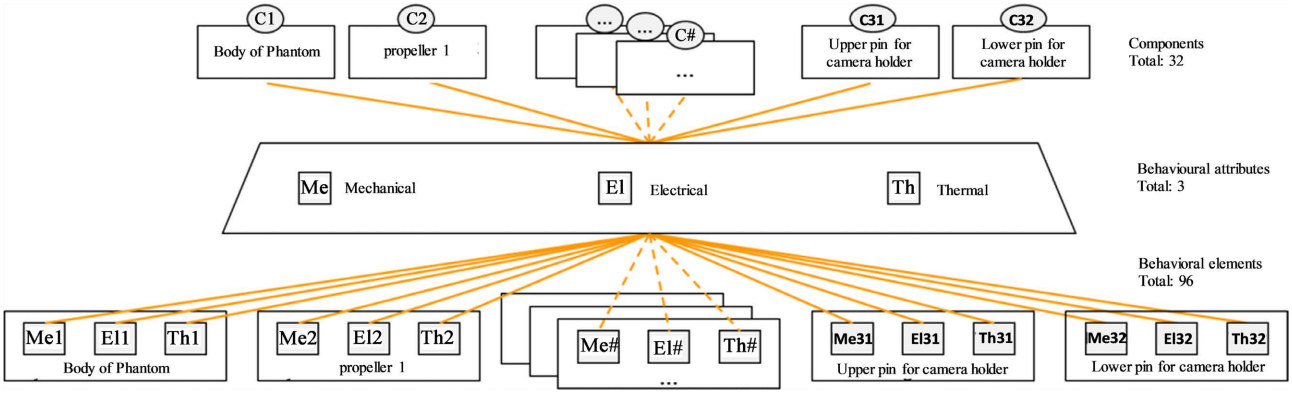

Figure 6. Determining the behavioral elements for the phantom drone.

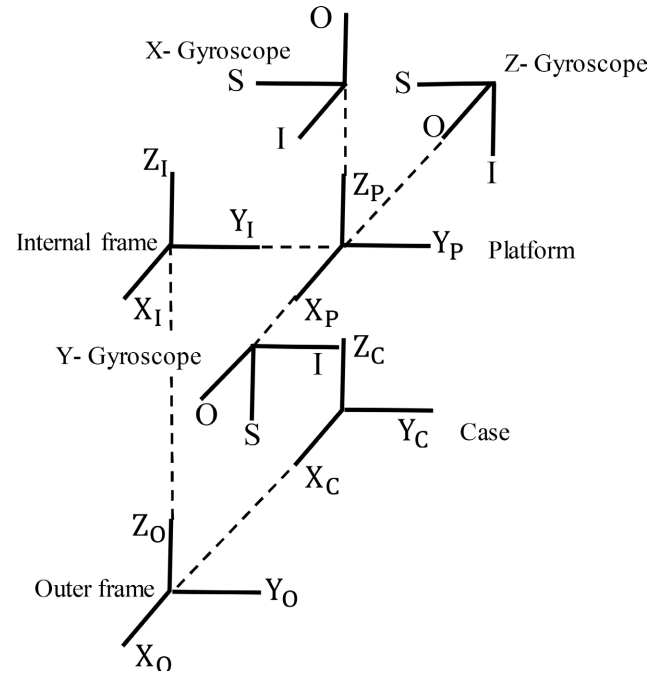

Figure 7. Relationships of all members of the 3-axis CGS.

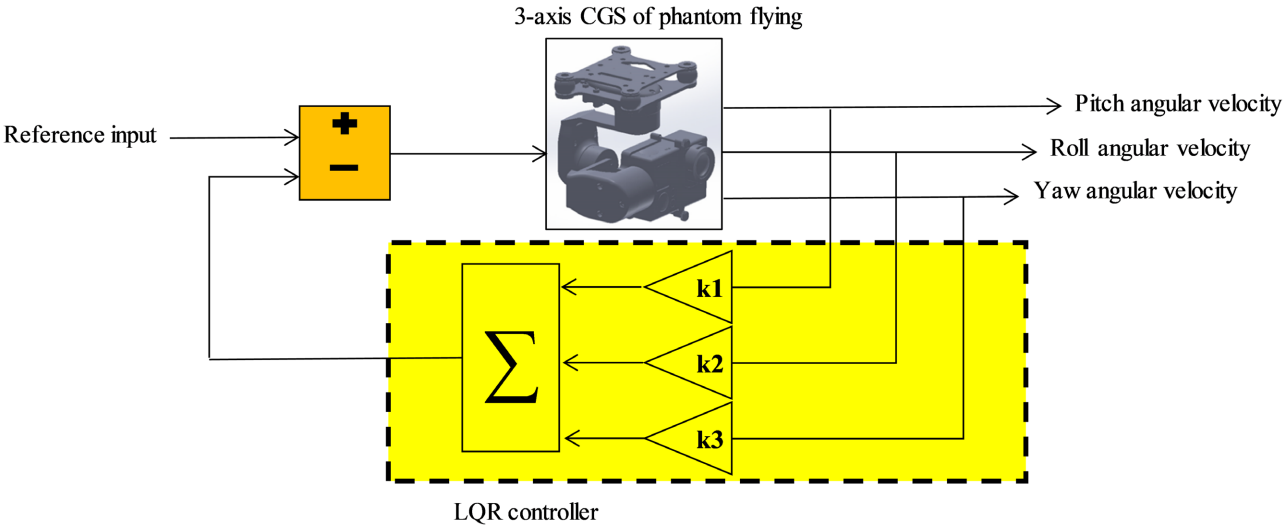

Figure 8. Block diagram of LQR controller of a 3-axis CGS Phantom drone.

way that it starts with the innermost member and progresses to the outermost member, the base (See **Figure 5(B)** & **Figure 5(C)**). **Figure 8** and **Figure 9** show the block diagram of a simulated linear model of a 3-axis CGS of a phantom drone in the presence of a Linear Quadratic Regulator (LQR) controller and a Proportional Integral Derivative (PID) controller. Highlights of the phantom 3-SE drone include professional positioning, a 4 K camera with 3-axis CGS, a flight time of 25 minutes, and an image transmission system with a range of 4 km. **Figure 10** shows the phantom 3-SE drone and **Figure 11** shows the camera and 3-axis CGS of the phantom drone. The phantom 3-SE drone is made in dimensions of 50 × 50 cm. The CGS is a device that eliminates the vibration of the

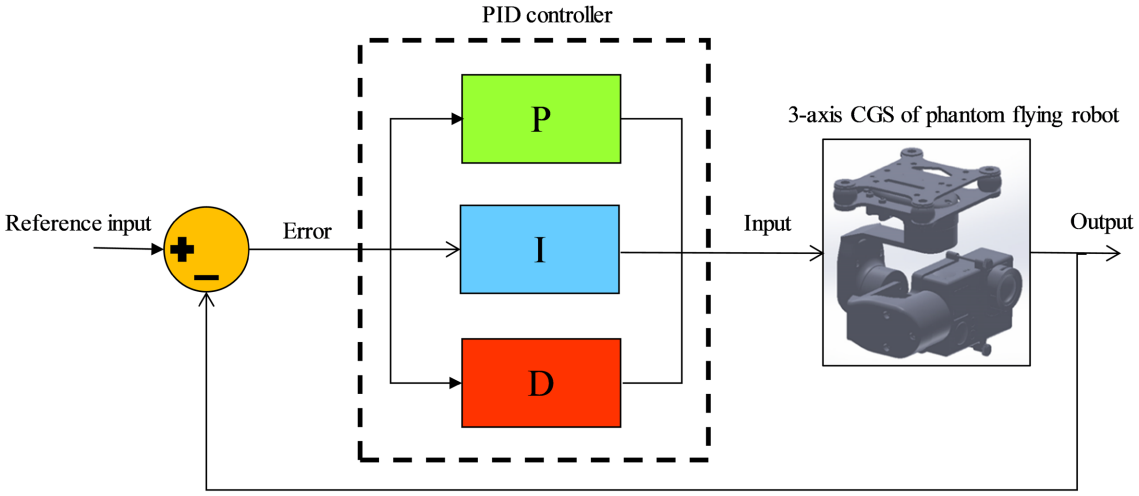

Figure 9. Block diagram of PID controller of a 3-axis CGS Phantom drone.

Figure 10. Phantom 3-SE drone.

Figure 11. Camera and 3-axis CGS of the phantom drone.

drone. In conventional drones that are not equipped with CGS, blurry photo will be a natural thing that can be annoying, even the mount of the camera cannot completely eliminates the vibration. The only device that can completely eliminate vibration is the CGS, which is available in 3 types: 1-axis, 2-axis and 3-axis. The CGS used in the phantom 3-SE drone is a 3-axis type, which is designed by DJI Company and is designed only for the phantom 3. It is important to note that even a slight shake can ruin the best shooting scenes. The 3-axis CGS designed for the phantom 3-SE assures the user that there will be no vibration in

her/his images and videos. During the flight, if the drone deviates in any direction, the CGS will stabilize the camera and will not allow the images to be shaken and recorded in a damaged way [9] [10].

The phantom drone is divided into 32 components. 16 of them are related to the phantom drone and 16 are related to the 3-axis CGS. **Figure 12** shows the product decomposition of the phantom drone with a 3-axis CGS. The BCDSM matrix has previously been demonstrated for a 3-axis CGS with a drone. Using this matrix, the execution procedure for a new change request is given below. According to the algorithm of **Figure 4**, after receiving the change request from the BCMC, the following activities are performed in the following order:

1) Development of a BCDSM Matrix

-Design phase: preliminary design

-Constraint level: behavioral attributes of components (mechanical, electrical and thermal)

2) Use the CAM software [14] to evaluate the sensitivity of the effects of change and identify the system parameters involved

Phantom Flying Robot Components

1- Body of phantom flying robot
2-Propeller 1
3- Propeller 2
4- Propeller 3
5- Propeller 4
6- Battery
7- Motor 1
8- Motor 2
9- Motor 3
10- Motor 4
11- Right skid
12- Left skid
13- Skid shock absorber 1
14- Skid shock absorber 2
15- Skid shock absorber 3
16- Skid shock absorber 4

3- axis GSP components

17- Upper plate
18- GSP shock absorber 1
19- GSP shock absorber 2
20- GSP shock absorber 3
21- GSP shock absorber 4
22- Lower plate (Case)
23- Yaw motor
24- Outer frame
25- Roll motor
26- Inner frame
27- Pitch motor
28- Platform
29- Camera
30- Camera holder
31- Upper pin of camera holder
32- Lower pin of camera holder

Figure 12. Product decomposition of the phantom drone with a 3-axis CGS.

-The 1st Part of CAM: development of sensitivity of all parameters to each other by functional simulation of subsystems.

-The 2nd part of CAM: calculating the range of first level changes of parameters to the requested change and calculating the range of second level changes of parameters to this change in subsystem algorithms.

-The 3rd part of CAM: integrating of changes in the design process using the Integrating coefficient index

The first result of using CAM software [14] to Change requested is CL = 2.

3) Send CAM software [14] information and BCDSM sensitivity by the BCMC to the relevant sections.

4) Calculate configuration management coefficients according to section 5.

5) Calculate the values of probability of the effect and the effect of time and cost POE = 9.6; TAC = 4 and confirmation of change is issued by BCMC.

6) **Figure 13** shows the algorithm for managing the change of requested behavioral attributes. This algorithm is a significant process to avoid a chain formation of multiple and divergent changes.

7) **Figure 14** shows the mechanical behavior change propagation model for

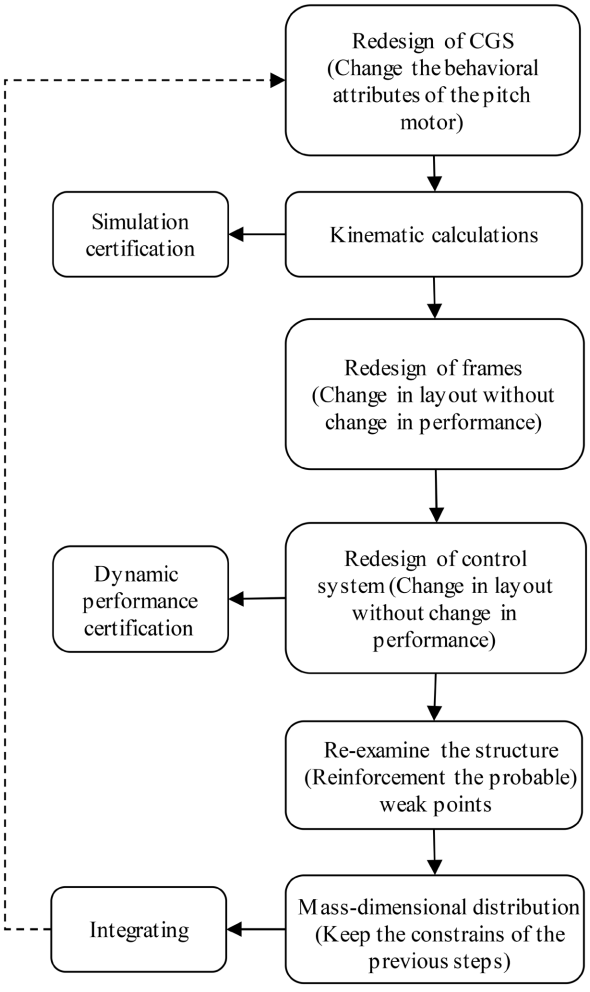

Figure 13. Algorithm for managing the change of requested behavioral attributes.

ID	Mechanical behavior	No.	1	2	3	4	5	6	7	8	9	10	11	12	13	14	15	16	17	18	19	20	21	22	23	24	25	26	27	28	29	30	31	32
Me1	Body of phantom flying robot	1						0.5	0.5	0.5	0.5	0.5	0.3	0.3					0.5															
Me2	Propeller 1	2							0.8																									
Me3	Propeller 2	3								0.8																								
Me4	Propeller 3	4									0.8																							
Me5	Propeller 4	5										0.8																						
Me6	Battery	6	0.5																															
Me7	Motor 1	7	0.5	0.8																														
Me8	Motor 2	8	0.5		0.8																													
Me9	Motor 3	9	0.5			0.8																												
Me10	Motor 4	10	0.5				0.8																											
Me11	Right skid	11	0.3												0.3	0.3																		
Me12	Left skid	12	0.3														0.3	0.3																
Me13	Skid shock absorber 1	13											0.3																					
Me14	Skid shock absorber 2	14											0.3																					
Me15	Skid shock absorber 3	15												0.3																				
Me16	Skid shock absorber 4	16												0.3																				
Me17	Upper plate	17	0.5																0.3	0.5	0.5	0.5	0.5											
Me18	GSP shock absorber 1	18																	0.3					0.3										
Me19	GSP shock absorber 2	19																	0.3					0.3										
Me20	GSP shock absorber 3	20																	0.3					0.3										
Me21	GSP shock absorber 4	21																	0.3					0.3										
Me22	Lower plate (Case)	22																		0.5	0.5	0.5	0.5		0.5									
Me23	Yaw motor	23																						0.5		0.8								
Me24	Outer frame	24																							0.8		0.5							
Me25	Roll motor	25																								0.5		0.8						
Me26	Inner frame	26																									0.8		0.5					
Me27	Pitch motor	27																										0.5		0.8				
Me28	Platform	28																											0.8		0.5		0.5	0.5
Me29	Camera	29																												0.5		0.5		
Me30	Camera holder	30																												0	0.5		0.5	0.5
Me31	Upper pin of camera holder	31																												0.5		0.5		
Me32	Lower pin of camera holder	32																												0.5		0.5		

Figure 14. Mechanical behavior change propagation model for 3-axis CGS and drone.

3-axis CGS and drone. Using the algorithm of Figure 13 and CAM software [14], the best model of propagation according to Figure 14 is obtained. This model is the result of the trade-off process of the parameter cycle in the design integrating cycle with the minimum change propagation index.

The mechanical behavioral property design structure matrix shown in Figure 14 is the densest behavioral property design structure matrix.

Figure 15 shows the balance of management for a part of behavioral change attributes of a 3-axis CGS and drone to request pitch motor (element 27) change in CAM software [14]. After integration of design parameters (integrating coefficient β), the change control α is performed and the results of the change control equilibrium for requesting the change of behavioral (mechanical) attribute in the pitch motor are obtained, according to Figure 15. This Figure shows the change propagation as a network [13]. In Figure 15, by considering a change initiator, the path of change propagation in other components can be followed. To find the optimal propagation probability for any desired path and to obtain the minimum process execution time, a GA is applied to the change process model. Figure 15 also shows that many changes in the complex engineering design process [8] of 3-axis CGS are interlinked and this makes it possible for designers determine the direction of change propagation it has been previously impossible through manual analysis [16].

3-axis CGS configuration management coefficients are shown in Table 2.

In a complex 3-axis CGS system [8], structural, behavioral, and functional attributes are intertwined. Whenever a design change occurs in one of the attributes of this complex system, the attributes of other components are also affected by

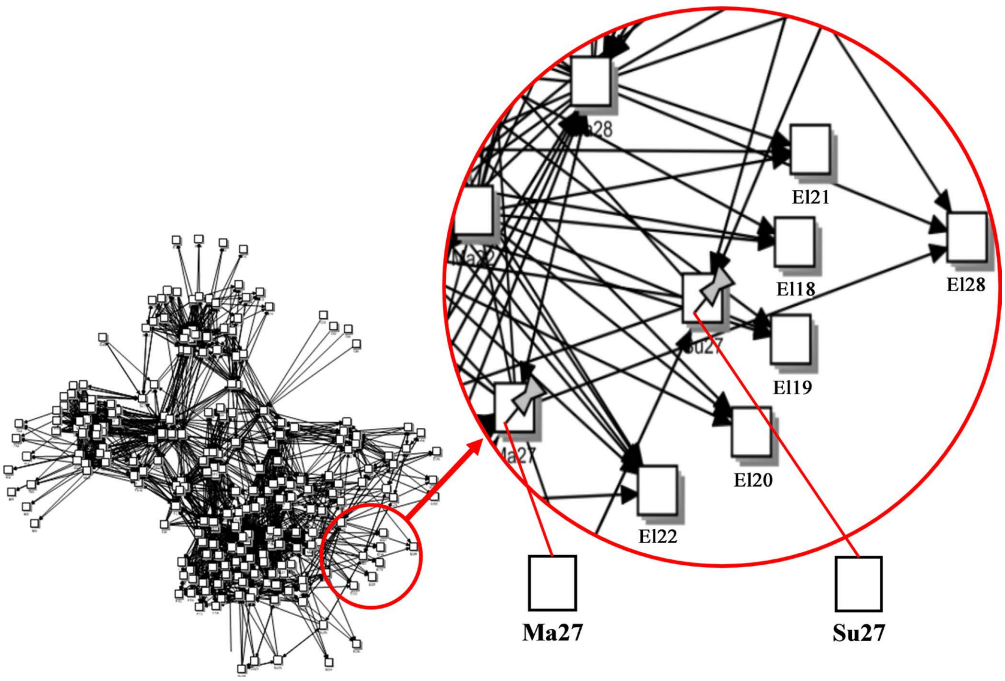

Figure 15. Balance of management for a part of behavioral change attributes of a 3-axis CGS and drone to request pitch motor (element 27) change in CAM software.

Table 2. 3-axis CGS configuration management coefficients.

No.	Coefficient name	Quality level	Quantification
1	Workload (total behavioral properties + complexity of matrix communication)	Level of subset = 1 Level of subsystem = 2 Level of Systemic convergence = 3 Level of Systemic non-convergent = 4	$a = 3$
2	Consumption resources (adding time + cost to the project)	Less than 0.1% = 1 Less than 1% = 2 Less than 5% = 3 More than 5% = 4	$b = 2$
3	Time spent by subgroups (change in project Gantt time)	No change = 1 Less than 0.1% = 2 Less than 5% = 3 More than 5% = 4	$c = 2$
4	Improve of requirements	No impact = 1 Positive impact = less than 1 Low negative impact = 2 High negative impact = 3 High change in a main requirement = 4	$d = 0.8$
5	Exigent	Removable in the range of resources = less than 1 Irreversible in the range of resources = More than 1	$f = 1$

that change [8]. Therefore, it would be important to understand the further changes propagation to redesign this product. In summary, first, the observation of the attributes change starts from the BCDSM matrices to show all the relationships between the attributes of this product. Second, the attribute of each component is analyzed to quantify probability and impact value with management through a checklist [7]. Values indicate that how useful or risky the behavioral attributes of a component are in terms of change. The system dynamics are implemented to plot complex relationships and change current [8]. This paper presents a new and efficient approach to managing changes in the design process of a 3-axis CGS to stabilize the camera mounted on a drone. This approach has been developed using systems engineering theory to enhance the behavior design process of 3-axis CGS. Therefore, designers can understand how to change the behavioral attributes of a 3-axis CGS and then redesign it to meet new requirements. To design the 3-axis CGS behavior with the aim of minimizing change propagation, the change propagation index (*CPI*) is introduced as follows [7]:

$$CPI_i = \sum_{j=1}^{N} \Delta E_{i,j} - \sum_{k=1}^{N} \Delta E_{i,k} = \Delta E_{out,i} - \Delta E_{in,i} \tag{3}$$

In which N is the number of behavioral attributes of the system elements and $\Delta E_{i,j}$ is a binary matrix (0, 1) which shows that the behavioral attributes of element i have changed due to a change in the behavioral attributes of element j. Here, the CPI has helped classify the behavioral attribute of the elements in terms of their relationship to change. Thus, the behavioral attributes of an element with $CPI > 0$ multiplies change, the behavioral attribute of an element with $CPI = 0$ carries change, and the behavioral attribute of an element with $CPI < 0$ absorbs change. The sum of the changes applied by all N elements, including the self-variable changes in element i with in-degree and the sum of the values of change applied from element i to all other $N - 1$ elements by out-degree is shown and the change propagation index is calculated as the following is simplified to a number between −1 and +1.

$$CPI(i) = \frac{C_{out}(i) - C_{in}(i)}{C_{out}(i) + C_{in}(i)} \tag{4}$$

Here, a value of +1 for the behavioral attribute of each element represents a complete multiplier of change. It means that a change in the behavioral attributes of that component, only effects the behavioral attributes of other components and has not any change itself. Value −1 for each element represents a complete absorber of a change. That is, the component absorbs only changes in behavioral attributes but does not make or transfer a change by itself. As expected, most elements have a combination of input and output changes which provide weak multipliers. Elements with zero or near zero CPI can be assumed as carriers of change.

A combination of data and different methods of displaying and interpreting this data, including the use of network image [13], BCDSM using CAM software [14] to visualize the propagation of behavioral changes, was described formerly.

For design of a 3-axis CGS with the goal of minimizing the propagation of behavioral changes, another index called clustering coefficient (CLC) is introduced as follows:

$$C_i = \frac{\left|\left\{e_{jk} : v_j, v_k \in N_i, e_{jk} \in E\right\}\right|}{k_i(k_i - 1)} \tag{5}$$

where v_k and v_j represent the behavioral elements k and j respectively. E is the set of connecting edges between the behavioral elements V, and k_i represents the number of elements. e_{jk} is an edge that connects the behavioral element j to the behavioral element k. N_i is a neighborhood for a behavioral element v_i that is closely attached to adjacent behavioral elements as follows:

$$N_i = \left\{v_j : e_{ij} \in E \vee e_{ji} \in E\right\} \tag{6}$$

To design a 3-axis CGS with the aim of finding the shortest path for the propagation of behavioral changes, another index called the between ness centrality coefficient (BNCC) is introduced [5]. The BNCC for measuring the centrality of a behavioral element among other behavioral elements is based on the

shortest paths and is introduced as follows [5]:

$$g(v)=\sum_{s\neq v\neq t}\frac{\sigma_{st}(v)}{\sigma_{st}} \tag{7}$$

where σ_{st} is the total number of shortest paths from the behavioral element *s* to the behavioral element *t*. $\sigma_{st}(v)$ is the number of paths that pass through the behavioral element *v*. The BNCC for a behavioral element is scaled by the number of pairs of behavioral elements, which is also presented as a sum of indicators. Therefore, the calculation is divided by dividing the number of pairs of behavioral elements without taking into account the behavioral element *v*, so that the number corresponding to *g* is in the range [0, 1]. The number of pairs of behavioral elements with $(N-1)(N-2)$ it shows that N is the number of large behavioral elements. It should be noted that this scale is intended for the highest possible value of *g*, where a behavioral element has crossed each of the shortest single paths [5]. In practice normalization without loss of accuracy is performed as follows:

$$normal\left(g(v)\right)=\frac{g(v)-\min(g)}{\max(g)-\min(g)} \tag{8}$$

Which eventually leads to:

$$\begin{aligned}\max(normal)&=1\\ \min(normal)&=0\end{aligned} \tag{9}$$

3. Results and Discussion

Tables 3-5 show the *CPI* for the entire set of elements (behavioral attributes).

By calculating the *CPI*, the system elements are sorted in a domain associated with the real number set {−1, +1} in which −1 stands for highest degree of absorbance and +1 shows the highest level of multiplication. Elements in the range $0.4 < CPI < 1$ are strong multipliers of the behavioral change (mechanical, electrical, and thermal) of 3-axis CGS. By calculating the *CPI*, the elements of the system can be shown on the absorber to multiplier the change in the range of −1 to +1 as shown in Figure 16.

Since scaling has always been done from a smaller range to a larger one, there will be no loss of accuracy (Tables 6-8).

To design a 3-axis CGS with the aim of accessing the special behavioral elements, in order to better management of propagation of behavioral changes, another index called reachability coefficient (RC) has been introduced. RC refers to the ability to move from one behavioral element to another (Tables 6-8).

In Tables 6-8 the CLCs show how much the behavioral elements of the CGS design matrix tend to come together. The high CLC for each behavioral element indicates that its subsystem components are highly linked to that subsystem, but they have little to do with other subsystems.

By calculating CLC, BNCC and RCs, for the behavioral elements of the system, they can be shown on separate spectra for mechanical, electrical and ther-

mal behaviors as shown in Figure 17.

Table 3. *CPI* value for the mechanical behavioral attributes elements of 3-axis CGS.

No.	Component Name	$C_{in}(i)$	$C_{out}(i)$	*CPI*
1	Me1	45	9	−0.67
2	Me2	26	2	−0.86
3	Me3	26	2	−0.86
4	Me4	26	2	−0.86
5	Me5	26	2	−0.86
6	Me6	4	1	−0.6
7	Me7	27	4	−0.74
8	Me8	27	4	−0.74
9	Me9	27	4	−0.74
10	Me10	27	4	−0.74
11	Me11	24	3	−0.78
12	Me12	24	3	−0.78
13	Me13	20	2	−0.82
14	Me14	20	2	−0.82
15	Me15	20	2	−0.82
16	Me16	20	2	−0.82
17	Me17	26	24	−0.04
18	Me18	20	9	−0.38
19	Me19	20	9	−0.38
20	Me20	20	9	−0.38
21	Me21	20	9	−0.38
22	Me22	24	13	−0.3
23	Me23	11	14	0.12
24	Me24	11	15	0.15
25	Me25	11	13	0.08
26	Me26	11	14	0.12
27	Me27	11	12	0.04
28	Me28	13	13	0
29	Me29	13	8	−0.24
30	Me30	14	3	−0.65
31	Me31	12	2	−0.71
32	Me32	11	2	−0.69

Table 4. *CPI* value for the electrical behavioral attributes elements of 3-axis CGS.

No.	Component Name	$C_{in}(i)$	$C_{out}(i)$	*CPI*
1	El1	9	0	−1
2	El2	2	0	−1
3	El3	2	0	−1
4	El4	2	0	−1
5	El5	2	0	−1
6	El6	27	44	0.24
7	El7	20	10	−0.33
8	El8	20	10	−0.33
9	El9	20	10	−0.33
10	El10	20	10	−0.33
11	El11	4	0	−1
12	El12	4	0	−1
13	El13	2	0	−1
14	El14	2	0	−1
15	El15	2	0	−1
16	El16	2	0	−1
17	El17	6	12	0.33
18	El18	3	0	−1
19	El19	3	0	−1
20	El20	3	0	−1
21	El21	3	0	−1
22	El22	6	0	−1
23	El23	20	20	0
24	El24	3	0	−1
25	El25	20	19	−0.03
26	El26	3	0	−1
27	El27	20	18	−0.05
28	El28	3	0	−1
29	El29	20	11	−0.29
30	El30	4	0	−1
31	El31	3	0	−1
32	El32	3	0	−1

Table 5. *CPI* value for the thermal behavioral attributes elements of 3-axis CGS.

No.	Component Name	$C_{in}(i)$	$C_{out}(i)$	*CPI*
1	Th1	18	5	−0.57
2	Th2	3	0	−1
3	Th3	3	0	−1
4	Th4	3	0	−1
5	Th5	3	0	−1
6	Th6	5	29	0.71
7	Th7	6	3	−0.33
8	Th8	7	3	−0.4
9	Th9	7	3	−0.4
10	Th10	7	3	−0.4
11	Th11	8	0	−1
12	Th12	8	0	−1
13	Th13	4	0	−1
14	Th14	4	0	−1
15	Th15	4	0	−1
16	Th16	4	0	−1
17	Th17	12	12	0
18	Th18	6	0	−1
19	Th19	6	0	−1
20	Th20	6	0	−1
21	Th21	6	0	−1
22	Th22	12	2	−0.71
23	Th23	9	13	0.18
24	Th24	6	6	0
25	Th25	9	12	0.14
26	Th26	6	6	0
27	Th27	9	10	0.05
28	Th28	6	4	−0.2
29	Th29	11	4	−0.47
30	Th30	8	1	−0.78
31	Th31	6	1	−0.71
32	Th32	6	1	−0.71

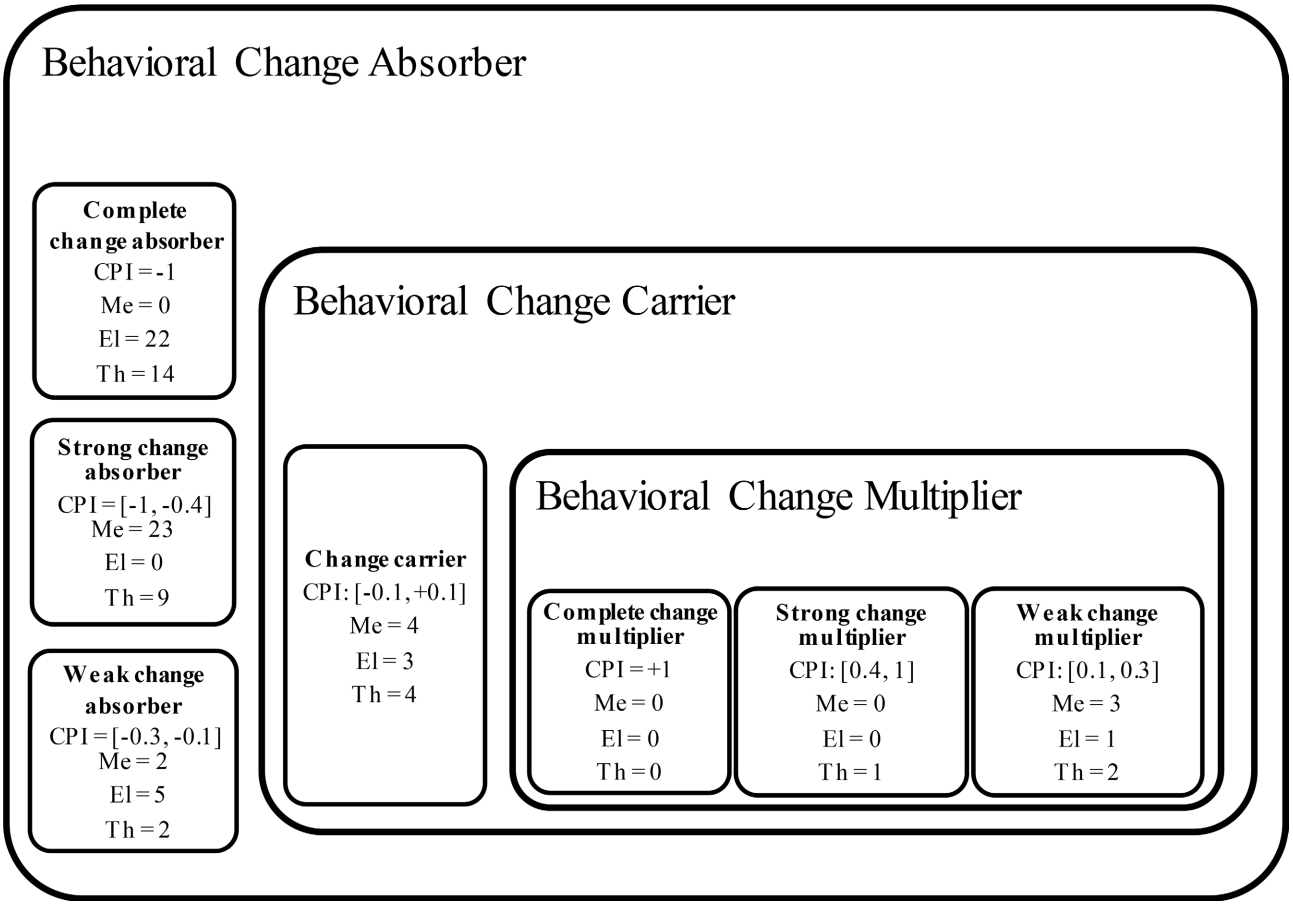

Figure 16. *CPI* range from -1 to +1 for the behavioral attributes of mapped elements for phantom CGS.

Table 6. CLC, BNCC and RCs for the mechanical behavioral attributes elements of 3-axis CGS.

No.	Component Name	CLC	BNCC	RC
1	Me1	0.153	2102.643	144
2	Me2	0.208	2.572	144
3	Me3	0.208	2.572	144
4	Me4	0.208	2.572	144
5	Me5	0.208	2.572	144
6	Me6	0.083	2.985	144
7	Me7	0.209	165.323	144
8	Me8	0.209	165.323	144
9	Me9	0.209	165.323	144
10	Me10	0.209	165.323	144
11	Me11	0.219	113.488	144
12	Me12	0.219	313.488	144
13	Me13	0.207	19.786	144

Continued

14	Me14	0.207	19.786	144
15	Me15	0.207	19.786	144
16	Me16	0.207	19.786	144
17	Me17	0.104	2285.417	144
18	Me18	0.172	230.468	144
19	Me19	0.172	230.468	144
20	Me20	0.172	230.468	144
21	Me21	0.172	230.468	144
22	Me22	0.189	1111.781	144
23	Me23	0.103	1063.137	144
24	Me24	0.111	1052.487	144
25	Me25	0.123	975.552	144
26	Me26	0.117	976.348	144
27	Me27	0.131	908.953	144
28	Me28	0.108	1003.449	144
29	Me29	0.152	208.952	144
30	Me30	0.275	33.902	144
31	Me31	0.242	40.117	144
32	Me32	0.2	567.434	144

Table 7. CLC, BNCC and RCs for the electrical behavioral attributes elements of 3-axis CGS.

No.	Component Name	CLC	BNCC	RC
1	El1	0.417	0	32
2	El2	1	0	32
3	El3	1	0	32
4	El4	1	0	32
5	El5	1	0	32
6	El6	0.106	1661.545	106
7	El7	0.387	54.963	106
8	El8	0.387	54.963	106
9	El9	0.387	54.963	106
10	El10	0.387	54.963	106
11	El11	0.667	0	32
12	El12	0.667	0	32
13	El13	1	0	32

Continued

14	El14	1	0	32
15	El15	1	0	32
16	El16	1	0	32
17	El17	0.131	38.911	32
18	El18	0.833	0	32
19	El19	0.833	0	32
20	El20	0.833	0	32
21	El21	0.833	0	32
22	El22	0.7	0	32
23	El23	0.203	202.644	106
24	El24	1	0	32
25	El25	0.22	150.062	106
26	El26	1	0	32
27	El27	0.232	145.4	106
28	El28	0.667	0	32
29	El29	0.356	81.027	106
30	El30	0.833	0	32
31	El31	1	0	32
32	El32	1	0	32

Table 8. CLC, BNCC and RCs for the thermal behavioral attributes elements of 3-axis CGS

No.	Component Name	CLC	BNCC	RC
1	Th1	0.172	207.656	64
2	Th2	0.333	0	64
3	Th3	0.333	0	64
4	Th4	0.333	0	64
5	Th5	0.333	0	64
6	Th6	0.07	358.616	65
7	Th7	0.208	63.321	65
8	Th8	0.208	63.321	106
9	Th9	0.208	63.321	106
10	Th10	0.208	63.321	106
11	Th11	0.286	0	64
12	Th12	0.286	0	64
13	Th13	0.333	0	64

Continued

14	Th14	0.333	0	64
15	Th15	0.333	0	64
16	Th16	0.333	0	64
17	Th17	0.105	122.61	64
18	Th18	0.367	0	64
19	Th19	0.367	0	64
20	Th20	0.367	0	64
21	Th21	0.367	0	64
22	Th22	0.242	33.465	64
23	Th23	0.102	181.567	106
24	Th24	0.167	18.138	64
25	Th25	0.124	91.945	106
26	Th26	0.167	12.902	64
27	Th27	0.134	95.381	106
28	Th28	0.222	14.599	64
29	Th29	0.17	257.803	106
30	Th30	0.361	5.29	64
31	Th31	0.381	2.645	64
32	Th32	0.381	2.645	64

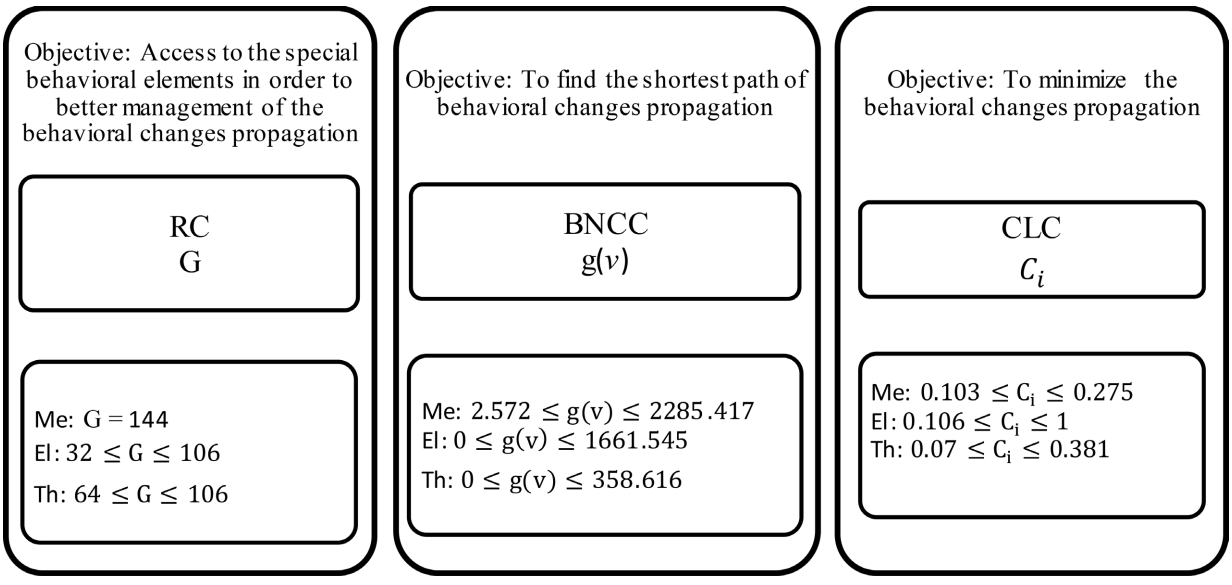

Figure 17. Range of Ci, g (v), G coefficients for behavioral elements of phantom CGS.

4. Conclusion

The main goal of the current research is to suggest a new approach for the iden-

tification of dependencies among a product's variables and to characterize them to predict the change impacts. A 3-axis CGS is modeled as a network of behavioral characteristics. The proposed process includes managerial decision-making and how to identify the best path for the process of change propagations in behavioral elements. The phantom sample drone with 32 components and 3 behavioral characteristics has been selected for each component. Half of which is related to the bird and the other half is related to the triangular gimbal. Behavioral links between elements are placed in a behavioral clustering design structure matrix (BCDSM). A constant change effect value is measured for all links and one of the three values, 0.3, 0.5 and 0.8 corresponding to low, medium and high probability of change, respectively, and is included in the matrices. In addition, a set of numerical indicators is created to help classify the various behavioral characteristics of the system as a receptor or reflector of change. By the criteria of "normal change propagation", "clustering coefficient", "degree of centrality", "reachability" and etc. through software code based on GA, change propagation analysis is performed. This method is implemented on a sample drone. The results, indicate that the absorption of change by behavioral elements is dominant in the mechanical (63.9%), electrical (61.1%) and thermal (38.9%) behaviors of the drone camera stabilizer system in redesign process. Therefore, it seems that the absorption of change by behavioral elements is dominant in the mechanical, electrical and thermal behaviors of the 3-axis CGS system. The importance of behavioral change absorbers is that they are best candidates for reducing or stopping the BCP. In general, behavioral change absorbers are also best candidates for reducing the cost of behavioral changes in the system and are desirable for the designer.

Conflicts of Interest

The authors declare no conflicts of interest regarding the publication of this paper.

References

[1] Anderson, D.M. (2014) Design for Manufacturability. 1st Edition, CRC Press, Boca Raton.

[2] Tang, D.B., Yin, L.L., Wang, Q., Ullah, I., Zhu, H.H. and Leng, S. (2016) Workload-Based Change Propagation Analysis in Engineering Design. *Journal of Concurrent Engineering: Research and Applications*, **24**, 17-34. https://doi.org/10.1177/1063293X15608510

[3] Smart-Tools-Lab (2005) Redesign IT: Managing Design Changes. http://www.engr.ucr.edu/~stahov/research/redesignit.htm

[4] Masmoudi, M., Leclaire, P., Zolghadri, M. and Haddar, M. (2017) Change Propagation Prediction: A Formal Model for Two-Dimensional Geometrical Models of Products. *Journal of Concurrent Engineering: Research and Applications*, **25**, 174-189. https://doi.org/10.1177/1063293X17698192

[5] Li, Y., Zhao, W. and Ma, Y. (2016) A Shortest Path Method for Sequential Change

Propagations in Complex Engineering Design Processes. *Journal of Artificial Intelligence for Engineering Design, Analysis and Manufacturing*, **30**, 107-121. https://doi.org/10.1017/S0890060415000311

[6] Zakeri, M., Nosratollahi, M., Sabeti, M.R., Moghadas Najaf Abad, H.R. and Maleki, H. (2021). A New Approach to Engineering Change Management for Space Projects. *Journal of Space Science & Technology*, **14**, 43-54.

[7] Plehn, C. (2018) A Method for Analyzing the Impact of Changes and Their Propagation in Manufacturing System. Dissertation, University of München, Munich.

[8] Li, Y. and Zhao, W. (2014) An Integrated Change Propagation Scheduling Approach for Product Design. *Journal of Concurrent Engineering: Research and Applications*, **22**, 347-360. https://doi.org/10.1177/1063293X14553809

[9] Moghadas, H.R., Jafari, H.R., Nikkhah, A. and Roshanian, J. (2009) Mathematical Modeling for a Three Axes Gyro Stabilized Platform. *Proceedings of the 8th International Conference of Iranian Aerospace Society, AERO*, 17-19 February 2009, MUT University, Munich.

[10] Nikkhah, A., Roshanian, J., Moghadas, H.R. and Jafari, H.R. (2014) Modeling and LQR Controller Design for a Three Axes Gyro Stabilized Platform. *Journal of Aerospace Mechanics*, **10**, 1-13.

[11] Eltaief, A., Borhen, L. and Remy, S. (2018) Associations Management and Change Propagation in the CAD Assembly. *Journal of Computers in Industry*, **98**, 134-144. https://doi.org/10.1016/j.compind.2018.02.012

[12] Duran-Novoa, R., Weigl, J.D., Henz, M. and Koh, E.C.Y. (2018) Designing in Young Organisations: Engineering Change Propagation in a University Design Project. *Journal of Research in Engineering Design*, **29**, 489-506. https://doi.org/10.1007/s00163-018-0292-9

[13] Walsh, H.S., Dong, A. and Tumer, I.Y. (2019) An Analysis of Modularity as a Design Rule Using Network Theory. *Journal of Mechanical Design*, **141**, 1-10. https://doi.org/10.1115/1.4042341

[14] Söderqvist, J.B., Lindlöf, L. and Trygg, L. (2019) Inter-Team Coordination in Agile Development: Learning from Non-Software Contexts. *Proceedings of the* 12*th International Workshop on Cooperative and Human Aspects of Software Engineering*, Montreal, 27/05/19, 69-70.

[15] Piccolo, S.A., Maier, A.M., Lehmann, S. and McMahon, C.A. (2019) Iterations as the Result of Social and Technical Factors: Empirical Evidence from a Large Scale Design Project. *Journal of Research in Engineering Design*, **30**, 251-270. https://doi.org/10.1007/s00163-018-0301-z

[16] Gräßler, I., Thiele, H., Oleff, C., Scholle, P. and Schulze, V. (2019) Method for Analysing Requirement Change Propagation Based on a Modified Pagerank Algorithm. *Proceedings of the* 22*nd International Conference on Engineering Design* (*ICED*19), Delft, The Netherlands, 5-8 August 2019.